Diversification of EPR signatures in Site directed spin labeling using a β-phosphorylated nitroxide

Note: The following files were submitted by the author for peer review, but cannot be converted to PDF. You must view these files (e.g. movies) online.

TOC.emf

PCCP Guidelines for Referees

Physical Chemistry Chemical Physics (**PCCP**) **is a high quality journal with a large international readership from many communities**

Only very important, insightful and high-quality work should be recommended for publication in *PCCP*.

To be accepted in *PCCP* - a manuscript <u>must</u> report:

- Very high quality, reproducible new work

- **Important new physical insights** of significant general interest

- A novel, stand-alone contribution

Routine or incremental work should <u>not</u> be recommended for publication. Purely synthetic work is not suitable for PCCP

If you rate the article as 'routine' yet recommend acceptance, please give specific reasons in your report.

Less than 50% of articles sent for peer review are recommended for publication in *PCCP*. The current PCCP Impact Factor is 3.83

PCCP is proud to be a leading journal. We thank you very much for your help in evaluating this manuscript. Your advice as a referee is greatly appreciated.

With our best wishes,

Philip Earis (pccp@rsc.org)   Prof Daniella Goldfarb
Managing Editor, PCCP   Chair, PCCP Editorial Board

General Guidance (For further details, see the RSC's Refereeing Procedure and Policy)

Referees have the responsibility to treat the manuscript as confidential. Please be aware of our **Ethical Guidelines** which contain full information on the responsibilities of referees and authors.

When preparing your report, please:
• Comment on the originality, importance, impact and scientific reliability of the work;
• State clearly whether you would like to see the paper accepted or rejected and give detailed comments (with references) that will both help the Editor to make a decision on the paper and the authors to improve it;

Please inform the Editor if:
• There is a conflict of interest;
• There is a significant part of the work which you cannot referee with confidence;
• If the work, or a significant part of the work, has previously been published, including online publication, or if the work represents part of an unduly fragmented investigation.

When submitting your report, please:
• Provide your report rapidly and within the specified deadline, or inform the Editor immediately if you cannot do so. We welcome suggestions of alternative referees.

The work presented in the article: CP-ART-11-2013-054816 - Diversification of EPR signatures in Site directed spin labeling using a β-phosphorylated nitroxide - combines the collaboration of different researchers having different field of expertises going from chemistry, biology, biophysics and theoritical calculations. This interdisciplinary study explains the rather large number of authors.

The contribution of each co-author is the following:

Spectroscopy & spectral simulation:
N. Le Breton: Performed EPR and CD experiments, performed the EPR spectral simulation E. Mileo: Performed EPR experiments A. Rockenbauer : Designed and supervised the EPR spectral simulation B. Guigliarelli: Designed the experiments M. Martinho and V. Belle: Designed and supervised the experiments and wrote the paper

Chemistry:
S. Marque: designed and supervised the synthesis of the new spin label K. Kabytaev: performed the synthesis of the new spin label

MD calculation:
J. Golebiowski: designed and supervised the MD calculations J. Topin: performed the MD calculations

Biology:
S. Longhi: designed and supervised the protein variants and partner protein D. Blocquel: purified the protein variants and partner protein J. Habchi: purified the protein variants and partner protein.

Journal Name

ARTICLE TYPE

Diversification of EPR signatures in Site directed spin labeling using a *β*-phosphorylated nitroxide

Nolwenn Le Breton[a], Marlène Martinho[a]*, Kuanysh Kabytaev[b], Jérémie Topin[c], Elisabetta Mileo[a], David Blocquel[d], Johnny Habchi[d], Sonia Longhi[d], Antal Rockenbauer[e], Jérôme Golebiowski[c], Bruno
5 Guigliarelli[a], Sylvain R. A. Marque[b], and Valérie Belle[a]*

Site Directed Spin Labeling (SDSL) combined to EPR spectroscopy is a very powerful approach to investigate structural transitions in proteins in particular flexible or even disordered ones. Conventional
10 spin labels are based on nitroxide derivatives leading to classical 3-lines spectra whose spectral shapes are indicative of the labels environment and thus constitute good reporters of structural modifications. However, the similarity of these spectral shapes precludes probing two regions of a protein or two partner proteins simultaneously. To overcome the limitation due to the weak diversity of nitroxide label EPR spectral shapes, we designed a new spin label based on a *β*-phosphorylated nitroxide giving 6-lines
15 spectra. This paper describes the synthesis of this new spin label, its grafting at four different positions of a model disordered protein able to undergo an induced α-helical folding and its characterization by EPR spectroscopy. For comparative purposes, a classical nitroxide has been grafted at the same positions of the model protein. The ability of the new label to report on structural transitions was evaluated by analyzing the spectral shape modifications induced either by the presence of a secondary structure stabilizer
20 (trifluoroethanol) or by the presence of a partner protein. Taken together the results demonstrate that the new phosphorylated label gives a very distinguishable signature which is able to report from subtle to larger structural transitions, as efficiently as the classical spin label. As a complementary approach, molecular dynamics (MD) calculations were performed to gain further insights into the binding process between the labeled N_{TAIL} and P_{XD}. MD calculations revealed that the new label does not disturb the
25 interaction between the two partner proteins and reinforced the conclusion on its ability to probe different local environments in a protein. Taken together this study represents an important step forward in the extension of the panoply of SDSL-EPR approaches.

Introduction

Since the pioneering works of the group of Hubbell,[1-2] Site
30 Directed Spin Labeling (SDSL) combined with Electron Paramagnetic Resonance (EPR) spectroscopy has emerged as a valuable tool for studying structural transitions in a wide range of proteins.[3-7] The conventional use of SDSL is based on the insertion of a paramagnetic label (nitroxide radical) at a cysteine
35 residue, most often introduced by site-directed mutagenesis and by its subsequent observation by EPR spectroscopy. The extreme sensitivity of the EPR spectral shape to the re-orientational motion of the nitroxide side chain arising from partial averaging of the anisotropic components (g- and hyperfine tensors) makes
40 this approach particularly well-suited to monitor conformational transitions induced by either protein-protein or protein-ligand interactions. In particular, SDSL has been shown to be a powerful and very sensitive tool to map induced folding events within intrinsically disordered proteins (IDPs) that are not readily

45 amenable to X-ray crystallography.[8-13]

However, applications of SDSL EPR spectroscopy are currently limited by the available commercial spin labels, such as 1-oxyl-2,2,5,5-tetramethyl-δ3-pyrroline-3-methyl (MTSL) or 3-maleimido-2,2,5,5-tetramethyl-1-pyrrolidinyloxy (referred to as
50 P) exhibiting typical three-lines EPR signatures of nitroxide radicals (Fig. 1). Whatever the regime of mobility of the spin label, the rather high similarity of the EPR spectral shapes precludes the study of different regions of a protein or two partner proteins simultaneously. Even if double labeling
55 strategies associated with Double Electron Electron Resonance (DEER) techniques are very informative to reveal structural changes in terms of inter-label distance measurements,[7, 14-15] this approach does not allow probing the local environment of each spin label individually and their potential modification
60 consecutive to structural changes. Nevertheless, the dynamic behavior of a protein often involves different regions, with the best known example being allostery, a mechanism by which ligand binding at one site influences binding at other sites through
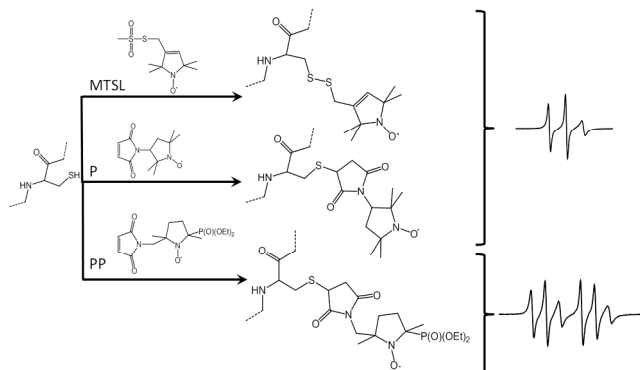
Fig. 1. Chemical structures of cysteine side-chain labeled with nitroxide radicals: 1-oxyl-2,2,5,5-tetramethyl-δ3-pyrroline-3-methyl methanethiosulfonate (MTSL), 3-maleimido-2,2,5,5-tetramethyl-1-pyrrolidinyloxy (P) and {2-(diethoxyphosphoryl)-5-[(2,5-dioxo-2,5-dihydro-1H-pyrrol-1-yl)methyl]-2,5-dimethylpyrrolidin-1-yl}oxidanyl (PP) with an illustration of the corresponding three or six-lines EPR signatures.

a propagated structural change within the protein.[16-17] It is thus of importance to develop new spin labels that would allow the observation of different protein regions simultaneously. To overcome the limitations due to the weak diversity of nitroxide EPR spectral shapes, we designed a new spin label based on a β-phosphorylated nitroxide having a phosphorus atom in the vicinity of the NO group. Cyclic and linear stable β-phosphorylated nitroxides have been synthesized and well-characterized by EPR since decades.[18-23] Spin trapping is the main application taking advantage of the strong coupling with the ^{31}P nucleus that has proven to be highly sensitive to the nature of the trapped radical.[24-25] Two types of hyperfine coupling of the unpaired electron are indeed present: a strong one with the I = ½ ^{31}P nucleus and a weaker one with the I = 1 ^{14}N nucleus (typical averaged values $\bar{A}_P = 5.0$ mT and $\bar{A}_N = 1.4$ mT) leading to a well-separated doublet of triplets spectrum as illustrated in Figure 1.

For SDSL application, it is necessary to functionalize the nitroxide moiety allowing the covalent grafting of the label on the protein using the reactivity of the sulfhydryl group of cysteine residues, most often introduced by site-directed mutagenesis. Typical functions able to react with sulfhydryl groups are thiosulfonate group (found in MTSL for example) forming a disulfide bond between the cysteine and the spin label or maleimido function (3-maleimido proxyl for example) leading to a thio-ether bond (Fig 1). For the new β-phosphorylated spin label, we choose the maleimido function because of the resistance of the resulting labeled protein to reducing agents (such as DTT) compared to MTSL-labeled protein where reducing conditions lead to immediate release of the spin label through disulfide bridge break. The new label: {2-(diethoxyphosphoryl)-5-[(2,5-dioxo-2,5-dihydro-1H-pyrrol-1-yl)methyl]-2,5-dimethylpyrrolidin-1-yl}oxidanyl, referred to as PP, for "phosphorylated proxyl" was prepared in 8 steps (Scheme 1). The first three steps were previously described.[26-28] Briefly, the maleimido spin label was prepared from the aziridine key-intermediate in four steps: azidation, hydrogenation, maleimido formation and oxidation to nitroxide PP (for details, see SI). As a consequence of the presence of two stereogenic centers, PP label can exist as one of four possible stereoisomers: two diastereoisomers, each in one of
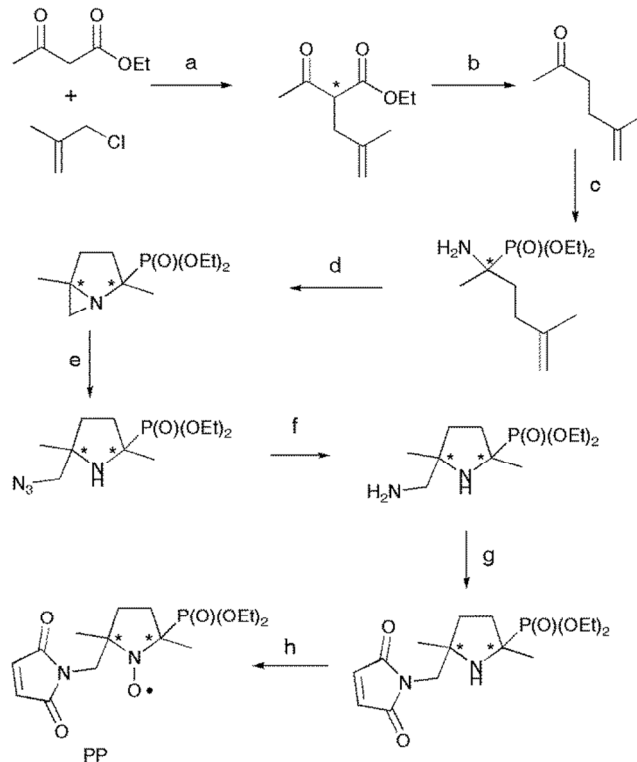
Scheme 1. Synthesis of spin label PP. (**a**) K$_2$CO$_3$, DMF, rt; (**b**) KOH, EtOH, 75 °C; (**c**) Diethylphosphite, NH$_3$, rt; (**d**) I$_2$, NaHCO$_3$, CH$_2$Cl$_2$, rt; (**e**) NaN$_3$, NH$_4$Cl, MeCN, 80 °C; (**f**) H$_2$, Pd/C, EtOH, rt; (**g**) rt (1) Maleic anhydride, (2) (COCl)$_2$ (**h**) m-CPBA, CH$_2$Cl$_2$, rt. Asterisks indicate asymmetric carbons.

two possible absolute enantiomeric configurations. It should be noted that during the synthesis (see SI for details), one diastereoisomer was lost. The two remaining enantiomers were used to complete the synthesis up to the maleimide substituted nitroxide. Room temperature EPR spectrum of PP gives a typical 6-lines spectrum with the following average hyperfine coupling values $\bar{A}_N = 1.4$ mT and $\bar{A}_P = 5.0$ mT (see Fig. S1). According to the McConnell equation[29-30] and to the data reported in the literature for β-phosphorylated nitroxides, diastereomeric nitroxides exhibit very similar nitrogen coupling constants but very different phosphorus ones. In our case, the unique value of phosphorus hyperfine coupling constant of PP confirms that only a couple of enantiomers is present.[21, 31-32] Compared to the classical 3-maleimido proxyl spin label P, the new label bears a supplementary methylene bridge between the maleimide and the nitroxide moieties but it should be noted that for both labels 6 chemical bonds separate the NO group from the S atom of the cysteine.

This study aims at evaluating the ability of PP to be a good reporter of structural changes within a model protein. The C$_{term}$ region of the Measles virus (MeV) nucleoprotein N$_{TAIL}$ (amino acids 400-525) was taken as an intrinsically disordered domain model undergoing a localized α-helical induced folding in the presence of its partner, the X domain of the phosphoprotein (P$_{XD}$).[33-35] This association has been particularly well-documented using SDSL EPR spectroscopy (with MTSL nitroxide) that allowed the precise mapping of the α-helical induced folding of N$_{TAIL}$ in the 488-502 region.[9-10] Four sites (407, 491, 496, 517) have been chosen for spin labeling to illustrate different behaviors of N$_{TAIL}$ either in the presence of a

secondary structure stabilizer (TFE, 2,2,2 trifluoroethanol) or in the presence of its partner protein P_{XD} in order to investigate the spin label response from small structural changes (TFE effect) to more important ones (partner induced folding). For sake of 5 comparison, the classical 3-maleimido proxyl P was grafted at the same positions and studied under the same conditions. Finally, molecular dynamic calculations were performed to bring complementary information on the binding process of labeled N_{TAIL} (either with P or PP) with P_{XD}.

10 Results and Discussion

Four MeV N_{TAIL} variants representative of four different spin label environments in the bound form were chosen for comparative purposes (Fig. 2a). It has been shown that position 407 is far away from the interaction site with P_{XD} and not affected 15 upon addition of the partner, positions 491 and 496 are within the
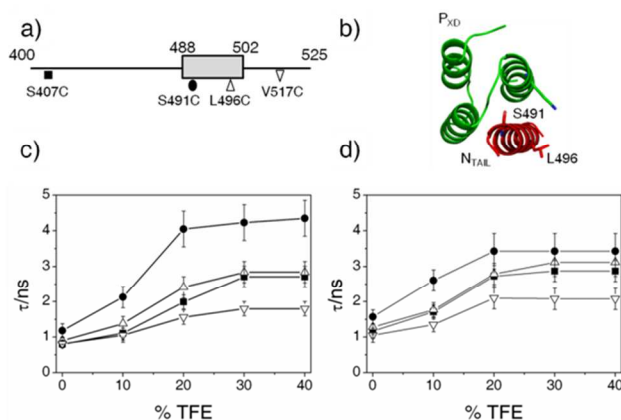

Fig. 2. (a) Schematic representation of positions targeted for spin labeling within N_{TAIL}, **(b)** Crystal structure of the MeV chimera between P_{XD} (green) and the N_{TAIL} region (red) encompassing residues 486–504 20 (pdb code 1T6O).[36] **(c, d)** Variation of the rotational correlation time τ (ns) as a function of increasing amount of TFE for S407C (squares), S491C (circles), L496C (up triangles) and V517C (down triangles) N_{TAIL} variants labeled with P **(c)** and PP **(d)**.

induced α-helix either pointing towards the partner (491) or being 25 solvent exposed (496) (Fig. 2b). Position 517 is in a region that does not undergo an α-helical transition but becomes more rigid upon binding to P_{XD}.[9, 12-13] N_{TAIL} variants were spin labeled through a two-step procedure consisting of a DTT reduction followed by covalent modification of the sulfhydryl group by 30 either P or PP nitroxide derivative (SI).

Structural transitions induced by TFE

In a first step, a study was performed aiming at comparing the ability of P and PP on reporting small structural changes induced

by the presence of a secondary structure stabilizer, the 2,2,2-35 trifluoroethanol (TFE). TFE mimics the hydrophobic environment experienced by proteins in protein-protein interactions and is therefore widely used to reveal the propensity of disordered regions to undergo an induced folding.[8, 37] The global structure of the labeled variants was checked out by 40 circular dichroïsm studies. The far-UV CD spectra of N_{TAIL} variants labeled with P or PP (referred to as $N_{TAIL}^{P/PP}$) quite well superimpose onto that of the *wt* and of unlabeled N_{TAIL} variants. They are all typical of unstructured proteins and show the N_{TAIL} propensity to fold in the presence of 20% of TFE (Fig. S2). These 45 results therefore indicate that neither the introduction of P nor that of PP impairs the ability of N_{TAIL} to undergo α-helical folding whatever the position of the spin label. EPR spectra of $N_{TAIL}^{P/PP}$ were recorded with increasing amounts of TFE ranging from 0% to 40% (v/v) (Fig. S3). It should be noted that the low-50 field triplet of PP (corresponding to $m_I(^{31}P) = +1/2$) is reminiscent of the spectrum of P and that similar deformation of this part of the spectrum compared to P occurs upon increasing TFE concentration. Variations of the EPR spectral shapes reflect changes in the dynamic of the spin label revealing structural 55 changes of the protein.[8-9] All EPR spectra were simulated using an extended version of the ROKI software[38] (see experimental section and Fig. S3). The magnetic parameters ($\tilde{g}$, $\tilde{A}_P$, $\tilde{A}_N$ tensors) were adjusted by simulating the Q-band EPR spectra of P and PP recorded in frozen solutions (Fig. S4). The simulation allows 60 obtaining the rotational correlation time τ as a function of TFE concentration (Fig. 2c and 2d). Below 20% (v/v), addition of TFE triggers a decrease in the mobility *i.e.* an increase of τ values for all $N_{TAIL}^{P/PP}$ variants as already reported using MTSL on the same biological system.[9] Addition of larger amount of TFE does not 65 have further effect on the mobility of the labels. The most pronounced effect is observed for the S491C N_{TAIL} variant with variations ranging from 1.2 to 4.4 ns for S491C^P and 1.6 to 3.4 ns for S491C^{PP}. The mobility of the radical bound at position 517 is only moderately affected by TFE ranging from 0.8 to 1.8 ns for 70 V517C^P and from 1.1 to 2.1 ns for V517C^{PP}. For positions 496 and 407, the variations of τ values are in between those previously mentioned. That TFE is able to promote a drop in the mobility of a spin label located outside the region of interaction with P_{XD}, namely position 407, has already been observed using 75 MTSL.[9-10] This observation likely reflects a local folding propensity that has been proposed to be related to a possible gain of structure induced by binding to other N_{TAIL} partners such as the nucleoprotein receptor NR.[9-10] All together these results show that even if the range of τ variations is slightly larger with P as 80 compared to PP, the new label is able to evidence subtle structural changes induced by TFE.
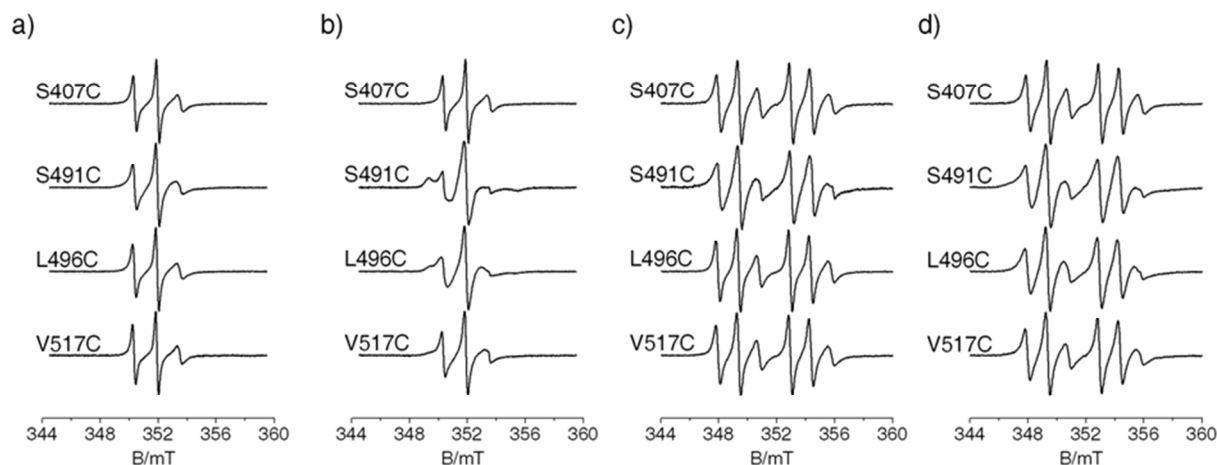
ARTICLE TYPE

Fig. 3. Amplitude normalized rt EPR spectra of N_{TAIL} variants labeled with P **(a, b)** and PP **(c, d)** without **(a, c)** or with **(b, d)** saturating amounts of P_{XD}, in 30% sucrose (w/v).

Structural transitions induced by the partner protein

5 To explore the efficiency of PP on monitoring folding events, EPR spectra of $N_{TAIL}^{P/PP}$ were recorded with saturating amounts of P_{XD} in the presence of 30% sucrose (w/v) (Fig. 3). Sucrose was used as a viscosity agent in order to minimize the contribution of global protein rotation to the EPR spectral shape.[39-40] Addition of

10 P_{XD} to S491C$^{P/PP}$ and L496C$^{P/PP}$ N_{TAIL} proteins triggers an important modification of the spectral shapes, in particular visible in the low field region of the spectrum (Fig. 3). The best agreement between experimental and calculated spectra was achieved by decomposing the EPR spectra into two different

15 components: one corresponding to N_{TAIL} bound to P_{XD} and one to unbound N_{TAIL}, a component always present despite the use of saturating amount of P_{XD}. This residual form of N_{TAIL} could correspond to a conformational sub-ensemble in which the spin label would adopt an orientation hampering binding to P_{XD}, as
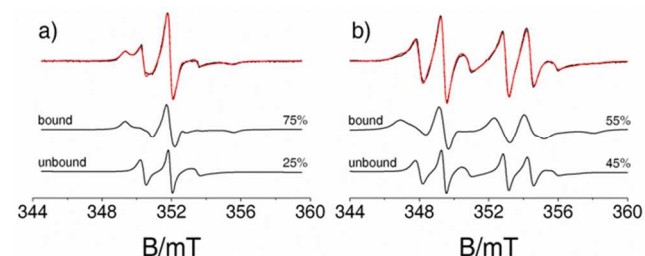
20 already observed.[9, 12]

Fig. 4. Amplitude normalized rt EPR spectra (black lines) of S491C^P **(a)** P and S491C^{PP} **(b)** in 30% sucrose (w/v). The simulated spectra (red lines) obtained using the ROKI[38] software are superimposed to the

25 experimental spectra. Amplitude normalized individual components corresponding to the bound and unbound forms are displayed with their respective proportion.

Figure 4 shows an example of such simulation for S491C$^{P/PP}$ (for L496C$^{P/PP}$ and V517C$^{P/PP}$, see Fig S5). Each component accounts

30 for ~50% except for S491C^P N_{TAIL}, where the unbound form counts for 25% and the bound form for 75% (Fig. 4 and Table 1).

Table 1. Rotational correlation time extracted from the simulation of the EPR spectra of N_{TAIL} variants labeled with P or PP in the presence of 30% (w/v) sucrose either in the absence or in the presence of saturating amount

35 of PXD.

		Free N_{TAIL}	N_{TAIL}-P_{XD} complex	
	variant	τ_{free} (ns)	τ_{bound} (ns)	% bound form
N_{TAIL}^P	S407C	2.0 (3)	2.0 (3)	100
	S491C	3.6 (5)	40 (8)	75 (5)
	L496C	2.5 (4)	26 (5)	55 (5)
	V517C	1.9 (3)	23 (5)	45 (5)
N_{TAIL}^{PP}	S407C	3.2 (4)	3.2 (4)	100
	S491C	5.3 (5)	35 (8)	55 (5)
	L496C	2.3 (4)	20 (5)	55 (5)
	V517C	2.8 (3)	18 (6)	45 (5)

Analyses of the mobility of P or PP in the bound forms according to spin label position are displayed in Figure 5. Globally the obtained profiles are very similar for N_{TAIL}^P and N_{TAIL}^{PP}. The

40 most reduced mobility is observed at position 491 corresponding to a spin label sterically restricted by the partner, whereas no spectral change is observed at position 407, known to remain disordered.[9] For position 496, the less reduced mobility of the label compared to position 491 is attributed to the solvent-

45 exposure of this amino acid according to the chimera structure of the P_{XD}-N_{TAIL} complex[36] (Fig. 2) as already detected using MTSL.[9] For position 517, known to acquire a gain of rigidity resulting from the P_{XD} α-helical induced folding taking place upstream, the variation of the mobility of the label (P or PP) is

50 larger than that observed using MTSL.[9] This difference can be

attributed to the different flexibility of the nitroxide side-chain in the case of the MTSL as compared to the maleimido function.
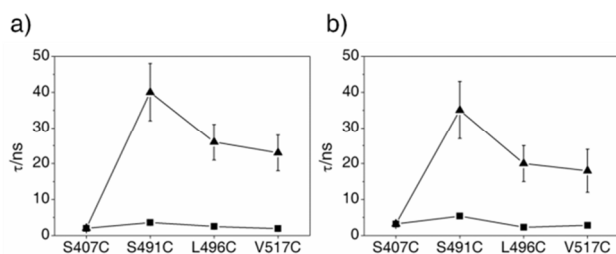

Fig. 5. Variation of the rotational correlation time τ (ns) of P **(a)** and PP
5 **(b)** spin labeled N_{TAIL} variants without (square) and with (triangle) saturating amounts of P_{XD} in 30% sucrose (w/v) as a function of spin label position.

Taken together, these results demonstrate that the newly synthesized β-phosphorylated nitroxide label is able to reveal a
10 wide range of structural modifications induced by partner binding with efficiency comparable to that of the classical maleimido proxyl.

Molecular dynamics calculations

MD is a powerful computational technique that has been proven
15 to be successful for describing molecular events and structural transitions in various biological systems.[41-43] As a complementary approach, we performed Molecular Dynamics (MD) calculations on models of the P_{XD}/N_{TAIL} chimera whose crystallographic structure was determined (PDB code 1T6O) to gain information
20 on the binding process between labeled N_{TAIL} and P_{XD} and to evaluate the eventual perturbation on complex formation induced by the presence of the label (see experimental section and SI for details). The chimera structures were modified with either P or PP at positions 491 or 496 of N_{TAIL} and were subjected to MD
25 calculations with explicit solvation. To get insights into the position of P or PP side-chains upon binding to P_{XD}, several unrestrained MDs with N_{TAIL} initially placed 5 Å away from P_{XD} but with different initial conditions were performed. It should be noted that, in the model, the free form of N_{TAIL} is taken α-helical
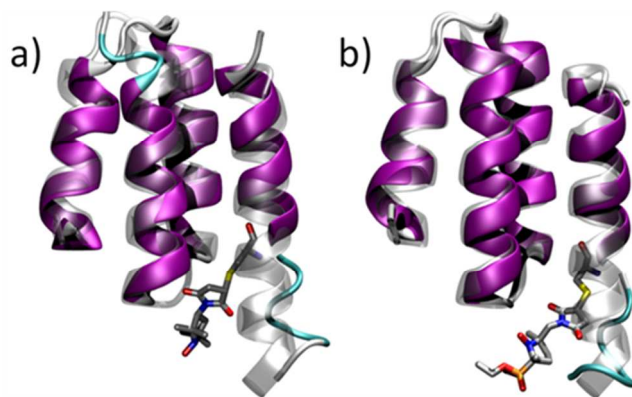30 which does not reflect the experimental condition where this segment is largely disordered.

Fig. 6. Typical calculated structure of P_{XD}/N_{TAIL} **(a)** S491C[P] and **(b)** S491C[PP]
sampled during the 100 ns MD. The calculated structures are
35 superimposed with the X-ray structures (in white). PP and P are shown in licorice. The colors are as follows: O: red; C: grey; N: blue, S: yellow, P: orange; α-helix: magenta; coil: blue.

We observed similar binding processes resulting in structures consistent with the restriction of mobility observed in the EPR
40 spectra recorded at these positions. For S491C[P/PP] N_{TAIL}, a typical bound structure was then considered for a further production MD of 100 ns. The influence of the label on the interaction between P_{XD} and N_{TAIL} is deemed rather minor. In S491C[P/PP] and L496C[P/PP], the binding process is indeed regulated by
45 hydrophobic contacts involving L473, L481, I504 residues in P_{XD} and L499 and M502 residues in N_{TAIL}, as observed on the wt N_{TAIL} experimental structure. As shown in Figure 6, in P_{XD} bound to S491C[P/PP], the distance between the two partners is not strongly affected, despite the large size of the modified cysteine
50 residue with both P and PP labels. Counter-intuitively, the size of the label (the molecular volumes of the cysteine, P and PP are 84, 300 and 400 Å[3], respectively) does not much affect the structure of the complex (Fig. S6 and S7). Hence, although PP is larger than P, its structure containing an additional methylene bridge
55 gives more flexibility to the label and there is a release of internal strain involving almost no change in the complexation process with P_{XD}. During the binding process, the side-chains of P or PP at position 491 adapt themselves to the interaction between N_{TAIL} and P_{XD} and adopt a convenient position, below the P_{XD} structure
60 (Fig. 6 and S8). In each case, the structure of N_{TAIL} remains folded as a helix, emphasizing minor perturbations of the *wt* fold, notably at the N-term side. Table 2 reports the computed atomic fluctuations of the oxygen atom of the nitroxide group, which quantifies the flexibility of the labels, either in the free N_{TAIL} or
65 bound to P_{XD}. These fluctuations for P and PP are similar in free N_{TAIL}, whatever their positions in the sequence. These results show that the flexibility of the labels is independent of both vicinal residues and label size. When bound to P_{XD}, the models accurately reproduce the decrease of mobility at position 491
70 observed through the EPR spectra analyses, the labels being in direct contact with P_{XD}. For this position, P and PP are both sensitive to complex formation and undergo a similar decrease of atomic fluctuations upon binding to P_{XD} (~7.5 Å→ ~3.0 Å, see Table 2). Position 496 is less sensitive to binding since this part
75 of N_{TAIL} is not in direct contact with P_{XD}. For PP, the decrease of the atomic fluctuations is observed at both 491 and 496 positions. For P, a similar decrease of flexibility is observed at position 491, but the model does not show any effect in the atomic fluctuations at position 496 upon binding to P_{XD}.

80 **Table 2** Atomic fluctuations (in Å) of the P and PP nitroxide moiety oxygen atom computed for the free N_{TAIL} and for N_{TAIL}-P_{XD} complex during 100 ns MDs.

	S491C		L496C	
	Free	Bound	Free	Bound
P	7.6	2.8	7.1	7.1
PP	7.5	3.1	7.1	4.3

Experimental

85 **Chemicals**

Unless otherwise noted, all chemicals and solvents were of analytical grade and used without further purification.

Synthesis of PP

Synthesis and full characterization are given in supplementary information.

Protein expression and purification

Cysteine-substituted N_{TAIL} variants were carried out as previously described.[9-10] Expression and purification of *wt* P_{XD} was performed as already described,[44] except that a washing step with 2M NaCl was added prior to elution from the immobilized metal affinity chromatography (IMAC) and that a nickel resin was used instead of cobalt resin.[45]

Labeling procedures

Before spin labeling, dithiothreitol (DTT) was added to each purified N_{TAIL} variant (approximately 1.5 mg) in a molar excess of 1:100. The mixture was incubated for 30 min in an ice bath to reduce the unique free cysteine residue. DTT was removed by PD10 desalting column (GE Healthcare) using a 10 mM MES, 150 mM NaCl at pH 6.5 as elution buffer. The fractions containing the protein were pooled. Spin labels were immediately added to the sample at a molar excess of 10:1 using a spin label (P or PP) stock solution at 40 mM in acetonitrile. The reaction was carried out during 1 h in the dark in an ice bath, under gentle stirring and a continuous flow of argon to avoid oxidation. The excess of unbound spin label was removed by gel filtration as described above, except that 10 mM sodium phosphate at pH 7.0 was used as elution buffer. The fractions giving an EPR signal of labeled proteins were pooled and concentrated by ultrafiltration using a 5 kDa cutoff polyethersulfone membrane (Vivaspin, Sartorius). In the case of S491C variant labeled with PP, the best yield was obtained using the same labeling procedure in a glove box.

Circular Dichroïsm

Circular dichroism (CD) spectra were recorded on a Jasco 810 dichrograph using 1-mm-thick quartz cells in 10 mM sodium phosphate at pH 7 at 20 °C in 0% or 20% of TFE. CD spectra were measured between 190 and 260 nm at 0.2 nm/min and were averaged from three independent acquisitions. Mean ellipticity values per residue ($[\theta]_{MRW, \lambda}$) were calculated as $[\theta]_{MRW, \lambda} = m \times \theta_\lambda / ((N-1) \times 10 \times d \times c)$, where m is the molecular mass (Daltons), N is the number of residues (125 for all N_{TAIL} proteins), θ_λ is the measured ellipticity (in degrees) at wavelength λ, d is the path length (0.1 cm) and c is the protein concentration expressed in g/mL. The molecular mass (m) values are 14632 Da for N_{TAIL} *wt* and L496C, 14648 Da for S407C and S491C, and 14636 Da for V517C. Protein concentrations of 0.1 mg/mL were used.

EPR spectroscopy

EPR spectra were recorded at room temperature on an ESP 300E Bruker spectrometer equipped with an ELEXSYS super high sensitivity resonator operating at 9.9 GHz. The microwave power was 10 mW, the magnetic field modulation frequency and amplitude were 100 kHz and 0.1 mT, respectively. The concentration of labeled proteins was evaluated by double integration of the EPR signal recorded under non-saturating conditions and comparison with that given by a MTSL standard sample. Protein concentrations were either calculated using OD_{280} measurements and the theoretical absorption coefficients ε (mg/mL.cm) at 280 nm, as obtained using the program ProtParam at the ExPASy server, or measured using the Biorad protein assay (Bio-Rad Laboratories, Hercules, CA). The labeling yields were estimated by calculating the ratio between the concentration of labeled proteins and the total protein concentration. Labeling yields obtained with PP were comparable to the one obtained with P ranging from 50 to 100 %. Protein concentrations of 50 μM were used to record individual EPR spectra in the presence of 0 % to 40 % TFE (Fluka) (v/v) in 10 mM sodium phosphate at pH 7.0. Q-band EPR was performed on a Bruker ELEXSYS 500 spectrometer equipped with a ER5106QT cavity fitted to a CF935 Oxford Instrument cryostat. The spectra were recorded at 100K with a microwave power of 1 μW to avoid saturation and a magnetic field modulation amplitude of 0.25 mT.

EPR spectral shape simulations

EPR spectra were simulated using an extended version of the ROKI software,[38] so as to achieve a detailed description of the spin label mobility. The method is based on the fact that, even for isotropic spectra, the line width variation in the hyperfine patterns depends on the anisotropy of g- and hyperfine tensors and changes drastically as a function of the correlation time. The rotational tumbling is described by individual jumps characterized by the solution of modified Bloch equations for conformational exchanges between two sites. The integration for all orientations can well reproduce the line shapes for all cases going from slow, intermediate to fast motions.

Molecular dynamics

The starting structure was taken from the X-ray structure of the P_{XD}/N_{TAIL} chimera (PDB code 1T6O).[36] Mutants S491C and L496C were built *in silico* using Swiss-PdbViewer (aka DeepView) software,[46] by changing serine 491 or leucine 496 into cysteine. The protonation state of each residue was assigned with respect to physiological conditions by using the H++ server.[47-48] For each probe, four systems were built: i/ N_{TAIL} alone modified at position 491, ii/ N_{TAIL} alone modified at position 496, iii/ N_{TAIL} modified (with P or PP) at position 491, in the vicinity of P_{XD} (in this case, the modified N_{TAIL} (with P or PP) were manually translated by ~5 Å away from P_{XD} in order to avoid steric clashes between P_{XD} and the probe and to prepare unrestrained MDs dedicated to sample the binding event between the two sub-systems) and iv/ N_{TAIL} modified at position 496 bound to P_{XD} built from the X-Ray structure of the chimera. Molecular dynamic simulations were carried out with either sander or pmemd within the AMBER12 suite of programs.[*AMBER 12*, University of California, San Francisco][49] ff03 parameters were used for all amino-acids and gaff parameters were obtained with Antechamber for P and PP. P and PP charges were computed with the RED server. A fully solvated 100 ns production with NPT conditions was performed for each structure.

Conclusion

To overcome the limitations due to the poor spectral diversity of usual nitroxide spin labels for SDSL-EPR applications, we have developed a new spin label based on a *β*-phosphorylated nitroxide. Using a model protein, we showed that this label is able to monitor subtle structural changes induced by TFE and that

it is also very efficient in probing different structural environments and folding events induced by protein-protein interaction. Molecular calculations revealed that the new label does not perturb the interaction between the two partner proteins and reinforced the conclusion that it is able to discriminate between different local environments, as efficiently as classical spin labels. This diversification of spectral signatures of spin labels extends our recent developments of spin labels designed to allow grafting on tyrosine residues instead of cysteine ones.[50-51] Thus, the combination of these approaches will open new perspectives for the simultaneous study of two regions of a protein targeting both cysteine and tyrosine residues. This study represents an important step forward in the enlargement of the panoply of SDSL-EPR approaches.

Acknowledgment

Notes and references

[a] Aix-Marseille Université, CNRS, BIP UMR 7281, 31 Chemin J. Aiguier, 13402 Marseille Cedex 20, France. Fax: 00.33.4 9116 4097; Tel: 00.33.491164414; E-mail: belle@imm.cnrs.fr and mmartinho@imm.cnrs.fr.
[b] Aix-Marseille Université, CNRS, ICR UMR 7273, Avenue Escadrille Normandie-Niemen, 13397 Marseille Cedex 20, France.
[c] Université de Nice – Sophia Antipolis, Institut de Chimie de Nice UMR 7272, 28 Avenue Valrose 06108 Nice, Cedex 2, France.
[d] Aix-Marseille Université, CNRS, AFMB UMR 7257, 163 Avenue de Luminy, 13288 Marseille Cedex 09, France.
[e] Research Centre of Natural Sciences, Institute of Molecular Pharmacology, P.O. Box 17, H-1525 Budapest, Hungary.
† Electronic Supplementary Information (ESI) available: Experimental procedures, experimental conditions for label synthesis, EPR, circular dichroïsm spectroscopy and MD calculations. See DOI: 10.1039/b000000x/

1. C. Altenbach, S. L. Flitsch, H. G. Khorana and W. L. Hubbell, *Biochem.*, 1989, **28**, 7806-7812.
2. C. Altenbach, T. Marti, H. G. Khorana and W. L. Hubbell, *Science*, 1990, **248**, 1088-1092.
3. J. P. Klare and H. J. Steinhoff, *Photosynth. Res.*, 2009, **102**, 377-390.
4. G. E. Fanucci and D. S. Cafiso, *Curr. Opin. Struct. Biol.*, 2006, **16**, 644-653.
5. S. Longhi, V. Belle, A. Fournel, B. Guigliarelli and F. Carriere, *J. Pept. Sci.*, 2011, **17**, 315-328.
6. E. Bordignon, *Top. Curr. Chem.*, 2012, **321**, 121-157.
7. H. S. Mchaourab, P. R. Steed and K. Kazmier, *Structure*, 2011, **19**, 1549-1561.
8. N. L. Pirman, E. Milshteyn, L. Galiano, J. C. Hewlett and G. E. Fanucci, *Protein Sci.*, 2011, **20**, 150-159.
9. V. Belle, S. Rouger, S. Costanzo, E. Liquiere, J. Strancar, B. Guigliarelli, A. Fournel and S. Longhi, *Proteins*, 2008, **73**, 973-988.
10. B. Morin, J. M. Bourhis, V. Belle, M. Woudstra, F. Carriere, B. Guigliarelli, A. Fournel and S. Longhi, *J. Phys. Chem. B*, 2006, **110**, 20596-20608.
11. V. Belle, S. Rouger, S. Costanzo, S. Longhi and A. Fournel, in *Instrumental analysis of intrinsically disordered proteins*, eds. V. N. Uversky and S. Longhi, Wiley, 2010, pp. 131-169.
12. M. Martinho, J. Habchi, Z. El Habre, L. Nesme, B. Guigliarelli, V. Belle and S. Longhi, *J. Biomol. Struct. Dyn.*, 2013, **35**, 453-471.
13. A. Kavalenka, I. Urbancic, V. Belle, S. Rouger, S. Costanzo, S. Kure, A. Fournel, S. Longhi, B. Guigliarelli and J. Strancar, *Biophys. J.*, 2010, **98**, 1055-1064.
14. G. Jeschke, *Annu. Rev. Phys. Chem.*, 2012, **63**, 419-446.
15. M. Pannier, S. Veit, A. Godt, G. Jeschke and H. W. Spiess, *J. Magn. Reson.*, 2000, **142**, 331-340.
16. K. Gunasekaran, B. Ma and R. Nussinov, *Proteins*, 2004, **57**, 433-443.
17. N. M. Goodey and S. J. Benkovic, *Nat Chem Biol*, 2008, **4**, 474-482.
18. S. Grimaldi, J. P. Finet, F. Le Moigne, A. Zeghdaoui, P. Tordo, D. Benoit, M. Fontanille and Y. Gnanou, *Macromolecules*, 2000, **33**, 1141-1147.
19. L. Dembkowski, J. P. Finet, C. Frejaville, F. Lemoigne, R. Maurin, A. Mercier, P. Pages, P. Stipa and P. Tordo, *Free Radical Research Communications*, 1993, **19**, S23-S32.
20. P. Stipa, J. P. Finet, F. Lemoigne and P. Tordo, *J. Org. Chem.*, 1993, **58**, 4465-4468.
21. A. Mercier, Y. Berchadsky, Badrudin, S. Pietri and P. Tordo, *Tetrahedron Letters*, 1991, **32**, 2125-2128.
22. D. L. Haire, E. G. Janzen, G. M. Chen, V. J. Robinson and I. Hrvoic, *Magn. Reson. Chem.*, 1999, **37**, 251-258.
23. V. V. Khramtsov, *Curr. Org. Chem.*, 2005, **9**, 909-923.
24. C. Frejaville, H. Karoui, B. Tuccio, F. Le Moigne, M. Culcasi, S. Pietri, R. Lauricella and P. Tordo, *J. Med. Chem.*, 1995, **38**, 258-265.
25. J. Maury, L. Feray, S. Bazin, J. L. Clement, S. R. Marque, D. Siri and M. P. Bertrand, *Chemistry - A European Journal*, 2011, **17**, 1586-1595.
26. G. Rosini, E. Marotta, M. Petrini and R. Ballini, *Tetrahedron*, 1985, **41**, 4633-4638.
27. P. Baeckstrom, L. Li, I. Polec, C. R. Unelius and W. R. Wimalasiri, *J. Org. Chem.*, 1991, **56**, 3358-3362.
28. F. Lemoigne, A. Mercier and P. Tordo, *Tetrahedron Letters*, 1991, **32**, 3841-3844.
29. H. M. McConnell, *J. Chem. Phys.*, 1956, **24**, 764.
30. H. M. McConnell and D. B. Chesnut, *J. Chem. Phys.*, 1958, **28**, 107.
31. A. Rockenbauer, A. Mercier, F. LeMoigne, G. Olive and P. Tordo, *J. Phys. Chem. A*, 1997, **101**, 7965-7970.
32. E. G. Janzen and Y. K. Zhang, *J. Org. Chem.*, 1995, **60**, 5441-5445.
33. J. M. Bourhis, V. Receveur-Brechot, M. Oglesbee, X. Zhang, M. Buccellato, H. Darbon, B. Canard, S. Finet and S. Longhi, *Protein Sci.*, 2005, **14**, 1975-1592.
34. S. Longhi, V. Receveur-Brechot, D. Karlin, K. Johansson, H. Darbon, D. Bhella, R. Yeo, S. Finet and B. Canard, *J. Biol. Chem.*, 2003, **278**, 18638-18648.
35. D. Karlin, S. Longhi, V. Receveur and B. Canard, *Virology*, 2002, **296**, 251-262.
36. Q. X. Hua, W. H. Jia, B. P. Bullock, J. F. Habener and M. A. Weiss, *Biochem.*, 1998, **37**, 5858-5866.
37. A. Rockenbauer and L. Korecz, *App. Magn. Reson.*, 1996, **10**, 29-43.
38. V. P. Timofeev and V. I. Tsetlin, *Biophys. Struct. Mechan.*, 1983, **10**, 93-108.
39. H. S. Mchaourab, M. A. Lietzow, K. Hideg and W. L. Hubbell, *Biochem.*, 1996, **35**, 7692-7704.
40. R. L. Kingston, D. J. Hamel, L. S. Gay, F. W. Dahlquist and B. W. Matthews, *Proc. Nat. Acad. Sci. U. S. A.*, 2004, **101**, 8301-8306.
41. R. Salomon-Ferrer, D. A. Case and R. C. Walker, *Wiley Interdisciplinary Reviews-Computational Molecular Science*, 2013, **3**, 198-210.
42. M. Gajula, K. P. Vogel, A. Rai, F. Dietrich and H. J. Steinhoff, *BMC Genomics*, 2013, **14**.
43. S. Fiorucci, J. Antonczak and J. Golebiowski, in *Protein-protein complexes:Analysis, modelling and drug design*, ed. M. Zacharias, Ed. imperial Press, 2010.
44. J. M. Bourhis, K. Johansson, V. Receveur-Brechot, C. J. Oldfield, K. A. Dunker, B. Canard and S. Longhi, *Virus Res.*, 2004, **99**, 157-167.

45. D. Blocquel, J. Habchi, S. Costanzo, A. Doizy, M. Oglesbee and S. Longhi, *Protein Sci,* 2012, **21**, 1577-1585.
46. N. Guex and M. C. Peitsch, *Electrophoresis*, 1997, **18**, 2714-2723.
47. J. C. Gordon, J. B. Myers, T. Folta, V. Shoja, L. S. Heath and A. Onufriev, *Nucleic Acids Res*, 2005, **33**, W368-371.
48. R. Anandakrishnan and A. Onufriev, *J Comput Biol*, 2008, **15**, 165-184.
49. A. W. Gotz, M. J. Williamson, D. Xu, D. Poole, S. Le Grand and R. C. Walker, *J Chem Theory Comput*, 2012, **8**, 1542-1555.
50. M. Lorenzi, C. Puppo, R. Lebrun, S. Lignon, V. Roubaud, M. Martinho, E. Mileo, P. Tordo, S. R. Marque, B. Gontero, B. Guigliarelli and V. Belle, *Angew. Chem. Int. Ed. Engl.*, 2011, **50**, 9108-9111.
51. E. Mileo, E. Etienne, M. Martinho, R. Lebrun, V. Roubaud, P. Tordo, B. Gontero, B. Guigliarelli, S. Marque and V. Belle, *Bioconjugate Chem.*, 2013, **24**, 1110-1117.

Supporting Information

Diversification of EPR signatures in Site directed spin labeling using a *β*-phosphorylated nitroxide

Nolwenn Le Breton, Marlène Martinho*, Kuanysh Kabytaev, Jérémie Topin, Elisabetta Mileo, David Blocquel, Johnny Habchi, Sonia Longhi, Antal Rockenbauer, Jérôme Golebiowski, Bruno Guigliarelli, Sylvain R. A. Marque, and Valérie Belle*

Synthesis and characterization of spin label PP

Materials. All reactions were carried out in oven–dried glassware. All chemicals were purchased from Sigma-Aldrich and used as received. Flash column chromatography was performed using 63–200 μm silica gel (Merck). Thin–layer chromatography (TLC) was performed using 60 F–254 silica gel plates (Merck). Visualization of TLC plates was accomplished with UV light and iodine or ethanolic phosphomolybdic solution.

Physical measurements. ^{1}H, ^{13}C, ^{31}P NMR were measured on Bruker Avance-300 and Bruker Avance-400 NMR spectrometers. ^{1}H NMR and ^{13}C NMR spectra were referenced to the residual non-deuterated solvent peak. ^{31}P NMR chemical shift were given to an external reference (85% H_3PO_4). Chemical shifts are reported in ppm and coupling constants in Hz. High-resolution mass spectra were obtained on 3200 QTRAP or QStar Elite (Applied Biosystems SCIEX).

Synthesis scheme
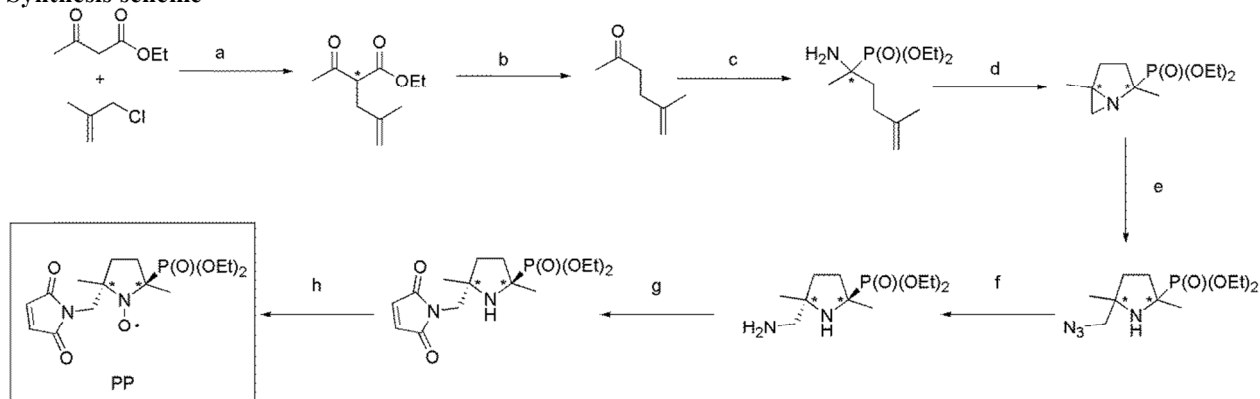
Synthesis of spin-label PP. (a) K_2CO_3, DMF, rt; (b) KOH, EtOH, 75 °C; (c) Diethylphosphite, NH_3, rt; (d) I_2, $NaHCO_3$, CH_2Cl_2, rt; (e) NaN_3, NH_4Cl, MeCN, 80 °C; (f) H_2, Pd/C, EtOH, rt; (g) rt *(1)* Maleic anhydride, *(2)* (COCl)$_2$ (h) *m*-CPBA, CH_2Cl_2, rt.

- **Ethyl 2-acetyl-4-methylpent-4-enoate**
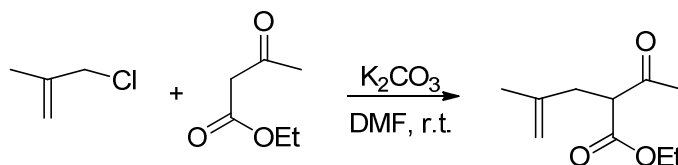
The title compound was prepared according to the procedure.[1] To a solution of ethyl 3-oxobutanoate (0.33 mol, 43 g) and 3-chloro-2-methylprop-1-ene (0.33 mol, 30 g) in 500 ml of DMF, anhydrous K_2CO_3 (1 mol, 138 g) was added. The reaction mixture was stirred at rt for 48 hours, then diluted with water and extracted with mixture of Et_2O/hexane (2:1). The organic solution was washed with water, brine, dried over $MgSO_4$ and evaporated. The crude product was purified by distillation at reduced pressure to give a colorless oil, 35 g, yield 58%. ^1H (400 MHz, $CDCl_3$) : 1.26 (t, J = 7.2 Hz, 3H), 1.73 (s, 3H), 2.24 (s, 3H), 2.55-2.58 (m, 2H), 3.66 (t, J = 7.6 Hz, 1H), 4.19 (q, J = 7.1 Hz, 2H), 4.69 (s, 1H), 4.78 (s, 1H).

- **5-methylhex-5-en-2-one**
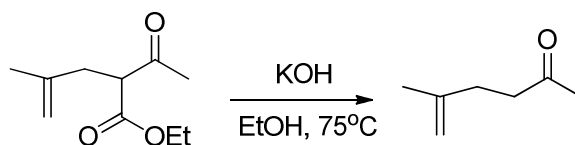
The 5-methylhex-5-en-2-one was prepared according to the procedure.[2] The ester (33 mmol, 6 g) was added to a solution of KOH (75 mmol, 4.2 g.) in 100 ml EtOH. The solution was stirred at 75 ^oC for 1 hour, neutralized with 10 % HCl and extracted with EtOAc. The combined organic phases were washed with brine, dried over $MgSO_4$ and concentrated to give a colorless oil, 3.1 g, yield 84 %. The obtained product was used in the next step without further purification. ^1H ($CDCl_3$, 400 MHz): 1.73 (s, 3H) ; 2.17 (s, 3H) ; 2.27-2.33 (m, 2H) ; 2.56-2.60 (m, 2H) ; 4.66 (s, 1H) ; 4.73 (s, 1H).

- **Diethyl (1-amino-1,4-dimethylpent-4-en-1-yl)phosphonate**
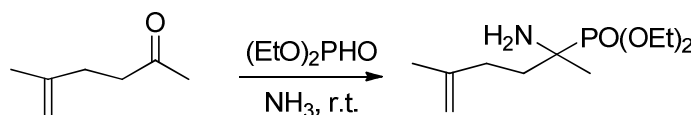
Diethyl (1-amino-1,4-dimethylpent-4-en-1-yl)phosphonate was prepared according to the procedure.[3] A stream of ammonia was bubbled through a mixture of ketone (20 mmol, 2.3 g.) and $(EtO)_2PHO$ (47 mmol, 6.5 g) at rt overnight. The reaction mixture was stirred with aqueous ammonia for 0.5 hour, diluted with chloroform and acidified with 10 % HCl. The aqueous solution was basified with $NaHCO_3$ and extracted with $CHCl_3$. The organic layers were dried over $MgSO_4$ and evaporated. Colorless oil, 3.5 g, yield 67%. It was used in the next step without further purification ^1H ($CDCl_3$, 400 MHz) δ: 1.20 (d, 3H, J = 16.1 Hz) ; 1.27 (t, 6H, J = 7.0 Hz) ; 1.42 (br. s, 2H, NH_2) ; 1.67 (s, 3H); 1.64-1.72 (m, 2H), 2.00-2.19 (m, 2H); 4.04-4.12 (quart, 4H, J = 7.2 Hz) ; 4.63 (s, 2H). ^{31}P: ($CDCl_3$, 120MHz) : δ = 31.5.

- **Diethyl (2,5-dimethyl-1-azabicyclo[3.1.0]hex-2-yl)phosphonate**
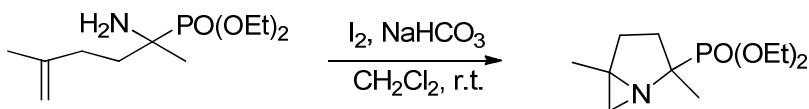
The aminophosphonate (5.68 g, 22.8 mmol) was dissolved in 50 mL of CH_2Cl_2, then 150 ml of 6 % solution of $NaHCO_3$ was added. A solution of I_2 (6.44 g, 25.4 mmol) in 150 mL of CH_2Cl_2 was added dropwise. The mixture was stirred at room temperature for 3 hours. Solid $Na_2S_2O_3$ was added to the reaction mixture and stirred for 30 minutes. The organic phase was decanted and the aqueous phase was extracted with CH_2Cl_2. The organic layers were collected, dried over $MgSO_4$, filtered and evaporated. The product was obtained as a mixture of two

diastereomers, colorless oil, 4.8 g, yield 85%. The product was used in the next step without further purification. ^{1}H NMR (CDCl$_3$, 400 MHz): 1.22-1.34 (m, 12H), 1.41-1.55 (m, 3H), 1.95-2.19 (m, 3H), 4.05-4.21 (m, 4H). ^{13}C NMR (CDCl$_3$, 75 MHz) : 16.4, 16.5, 16.5, 16.6, 19.8, 19.8, 21.0, 21.8, 23.8, 29.4, 29.5, 30.0, 30.1, 30.6, 30.8, 31.2, 32.7, 33.7, 33.7, 46.0, 46.2, 47.9, 61.6, 62.0, 62.1, 62.4, 62.5, 62.8, 64.5, 64.9, 66.7, 67.3. ^{31}P NMR (CDCl$_3$, 120 MHz): δ (ppm) = 29.9 (major) and 29.5 (minor). HRMS: calculated for C$_{11}$H$_{23}$NO$_3$P [M+H]$^+$ 248.1410, found: 248.1404.

- **Diethyl [5-(azidomethyl)-2,5-dimethylpyrrolidin-2-yl]phosphonate**
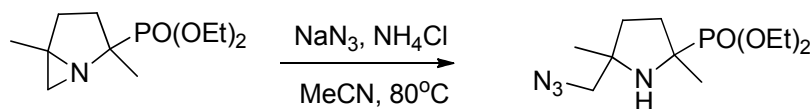
A solution of the aziridine (15 mmol, 3.7 g), NaN$_3$ (18.2 mmol, 1.18 g, 1.2 eq) and NH$_4$Cl (16.6 mmol, 0.89 g, 1.1 eq) in 95 ml MeCN was heated for 5 hours at 80°C. The reaction mixture was diluted with MeCN, filtered through Celite® and evaporated. The crude product was purified by column chromatography (eluent CH$_2$Cl$_2$/EtOH 95/5). The product was obtained as a mixture of diastereoisomers with the ratio 3:1, colorless oil, 2.4 g, yield 55%. Major diastereomer: ^{1}H NMR (CDCl$_3$, 400 MHz) 1.21 (s, 3H), 1.33 (t, J = 7.02, 6H), 1.37 (d, J = 15.29 Hz, 3H), 1.65-1.83 (m, 3H), 2.30-2.40 (m, 1H), 3.12-3.30 (m, 2H), 4.11-4.21 (m, 4H). ^{31}P NMR : (CDCl$_3$, 162 MHz) : δ (ppm) = 30.35. Minor diastereomer: ^{1}H NMR (CDCl$_3$, 400 MHz) 1.21 (s, 3H), 1.32 (t, J = 7.02 Hz, 6H), 1.39 (d, J = 15.29 Hz, 3H), 1.65-1.83 (m, 3H), 2.30-2.40 (m, 1H), 3.12-3.30 (m, 2H), 4.11-4.21 (m, 4H). ^{31}P NMR : (CDCl$_3$, 162 MHz) : δ (ppm) = 29.14. ^{13}C NMR (CDCl$_3$, 75 MHz): 16.4, 16.5, 16.6, 25.5, 25.6, 25.6, 26.2, 26.9, 33.9, 33.9, 34.4, 34.9, 35.0, 35.1, 59.7, 59.9, 61.3, 61.5, 61.5, 61.6, 62.0, 62.1, 62.6, 62.6, 63.4, 63.5. HRMS: calculated for C$_{11}$H$_{24}$N$_4$O$_3$P [M+H]$^+$ 291.1581, found 291.1580.

- **Diethyl [5-(aminomethyl)-2,5-dimethylpyrrolidin-2-yl]phosphonate**
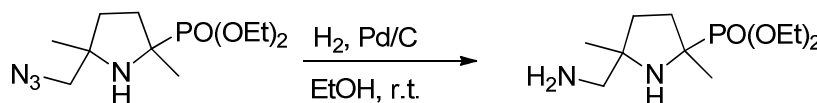
To a solution of the amine (2.6 mmol, 0.7 g) in 150 mL of EtOH 210 mg of Pd/C was added. The mixture was stirred for 6 hours under hydrogen atmosphere at rt. The reaction mixture was filtered through a Celite and evaporated. Only the major diastereomer was obtained as a yellowish oil (450mg, 71%). The obtained diamine was used in the next step without further purification. ^{1}H NMR : (CDCl$_3$, 400 MHz) : 1.14 (s, 3H), 1.33 (t, J = 7.24 Hz, 6H), 1.34 (d, J = 15.44 Hz, 3H), 1.66-1.78 (m, 3H), 2.14 (br. s, 3H), 2.30-2.39 (m, 1H), 2.49-2.61 (m, 2H), 4.11-4.22 (m, 4H). ^{13}C NMR (CDCl$_3$, 75 MHz): 16.2 (triplet like, J = 5.2 Hz, 2C), 25.4 (d, J = 8.1 Hz), 25.6, 34.1, 34.5 (d, J = 5.5 Hz), 51.5, 59.9 (d, J = 160.7 Hz), 61.7 (d, J = 7.7 Hz), 62.3 (d, J =7.7 Hz), 63.5 (d, J = 7.2 Hz). ^{31}P NMR: (CDCl$_3$, 162 MHz) : δ (ppm) = 31.0. HRMS: calculated for C$_{11}$H$_{26}$N$_2$O$_3$P [M+H]$^+$ 265.1676, found 265.1679.

- **Diethyl {5-[(2,5-dioxo-2,5-dihydro-1H-pyrrol-1-yl)methyl]-2,5-dimethylpyrrolidin-2-yl}phosphonate**
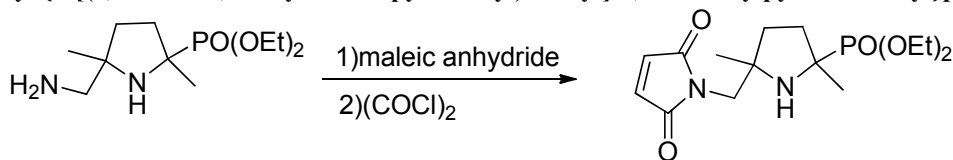
A toluene solution of the amine (2 mmol, 528 mg) and maleic anhydride (3 mmol, 300 mg) was stirred at rt overnight. The red oil deposited on the bottom of the flask was decanted, dissolved in dichloromethane and treated with oxalyl chloride (2 mmol, 255 mg). After stirring 24 h at rt the solution was washed with water, the aqueous layer was neutralized with NaHCO$_3$ and extracted with CHCl$_3$. The solvent was evaporated and the crude product was purified by column chromatography (eluent EtOH/Et$_2$O 1:4), 48 mg oil, yield 7 %. ^{1}H NMR (CDCl$_3$, 400 MHz) : 1.15 (s, 3H), 1.28 (d, J = 15.35 Hz, 3H), 1.31 (t, J = 7.09 Hz, 6H), 1.64-1.78 (m, 3H), 2.27-2.42 (1H, m), 3.52 (dd, J$_{A,B}$ = 14.05 Hz, 2H), 4.11-4.17 (dq, J$_1$ = 6.94 Hz, J$_2$ = 2.5 Hz, 4H), 6.74 (s, 2H). ^{13}C NMR (CDCl$_3$, 75 MHz): 16.5 (triplet like, J = 5.2 Hz, 2C), 25.1 (d, J = 8.8 Hz), 27.1, 34.0 (d, J = 1.1 Hz), 35.1 (d, J = 5.5 Hz), 47.8, 60.6 (d, J =

166.7 Hz), 62.2 (d, J = 7.7 Hz), 62.7 (d, J = 7.2 Hz), 64.1 (d, J = 8.3 Hz), 134.2 (2C), 171.4 (2C). ^{31}P NMR (CDCl$_3$, 162 MHz) : 30.0 ppm. HRMS: calculated for C$_{15}$H$_{26}$N$_2$O$_5$P [M+H]$^+$ 345.1574, found 345.1572.

- **{2-(diethoxyphosphoryl)-5-[(2,5-dioxo-2,5-dihydro-1H-pyrrol-1-yl)methyl]-2,5-dimethylpyrrolidin-1-yl}oxidanyl - PP**
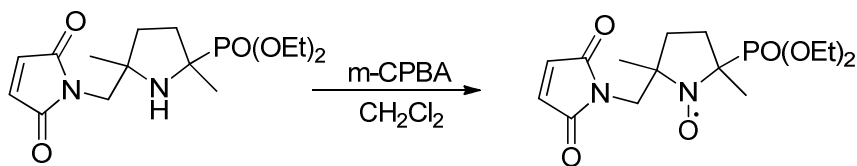
A solution of maleimide (0.029 mmol, 10 mg) and m-CPBA (0.058 mmol, 10 mg) in CH$_2$Cl$_2$ was stirred for 3 h at rt. The reaction mixture was washed with Na$_2$S$_2$O$_3$, NaHCO$_3$ then dried with MgSO$_4$. The solvent was evaporated and the crude product was purified by flash chromatography (eluent EtOAc/Et$_2$O 1/1). The nitroxyde was obtained as a yellowish oil (4.7 mg, yield 45 %) HRMS : calculated for C$_{15}$H$_{25}$N$_2$O$_6$P [M+H]$^+$ 360.1445, found 360.1442.
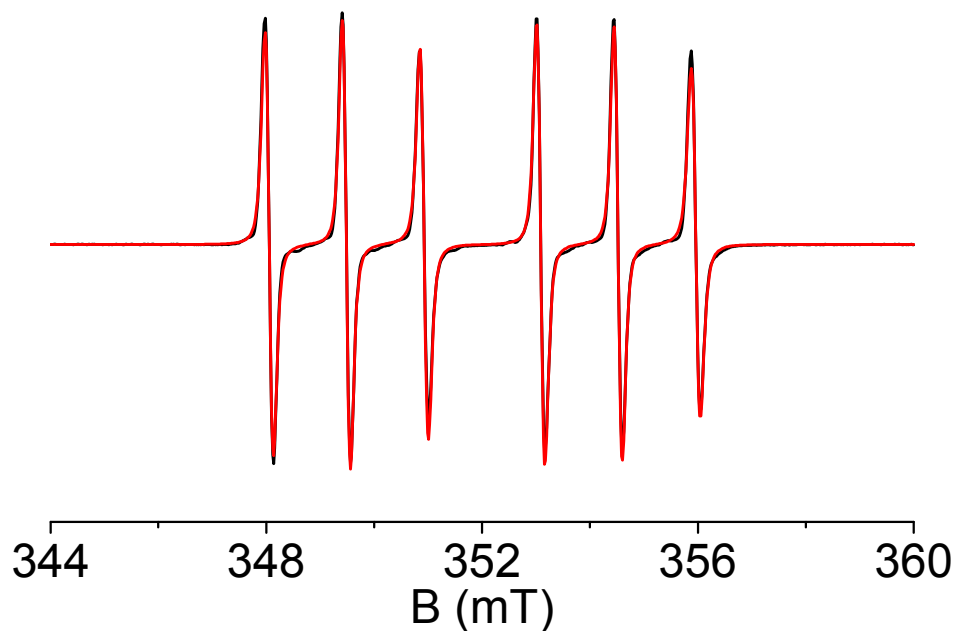
Figures

Figure S1. Experimental (black line) and simulated (red line) X-band EPR spectra of PP recorded at room temperature using a 200 μM solution in 10 mM sodium phosphate buffer at pH 7. The microwave power was 10 mW and the magnetic field modulation amplitude was 0.1 mT. Simulation was performed using ROKI software [4] with the following parameters: $g_\perp = 2.0069$, $g_{//} = 2.0021$, $A_{P\perp} = 4.7$ mT, $A_{P//} = 5.6$ mT, $A_{N\perp} = 0.7$ mT, $A_{N//} = 2.7$ mT $\tau = 0.17$ ns.
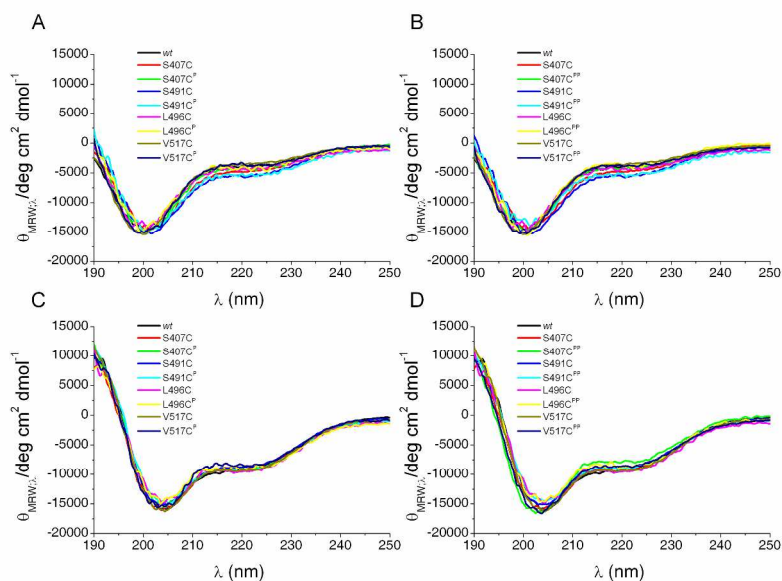

Figure S2. Far-UV CD spectra of wt, unlabeled variants and labeled $N_{TAIL}{}^{P}$ (left) and $N_{TAIL}{}^{PP}$ (right) variants at 0% **(A, B)** and 20% **(C, D)** TFE (v/v).
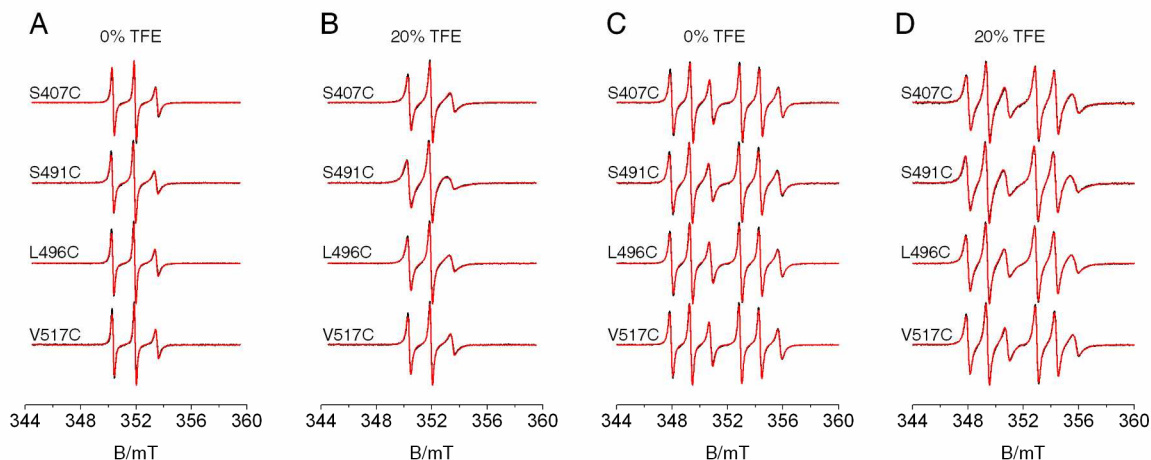
Figure S3. Amplitude normalized rt EPR spectra (black) of P **(A, B)** and PP **(C, D)** spin labeled N_{TAIL} variants in the presence of 0% **(A, C)** and 20 % **(B, D)** TFE (v/v). Simulated spectra (red) using ROKI software[4]are superimposed on the experimental spectra.
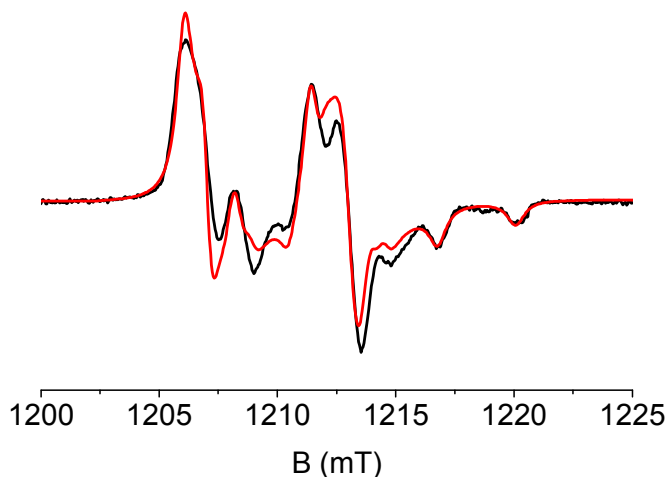

Figure S4. Experimental (black line) and simulated (red line) Q-band EPR spectra of S407C N_{TAIL}^{PP} variant, recorded at 100K using a 100 μM solution in the presence of 30% (v/v) glycerol in 10 mM sodium phosphate buffer at pH 7. The microwave power was 1 μW and the magnetic field modulation amplitude was 0.25 mT. Simulation was performed using ROKI software [4] with the parameters : g_{xx} = 2.0088, g_{yy} = 2.0059, g_{zz} = 2.0020, A_{Pxx} = 5.2 mT, A_{Pyy} = 5.7 mT, A_{Pzz} = 6.3 mT, A_{Nxx} = 0.4 mT, A_{Nyy} = 0.6 mT, A_{Nzz} = 3.3 mT.
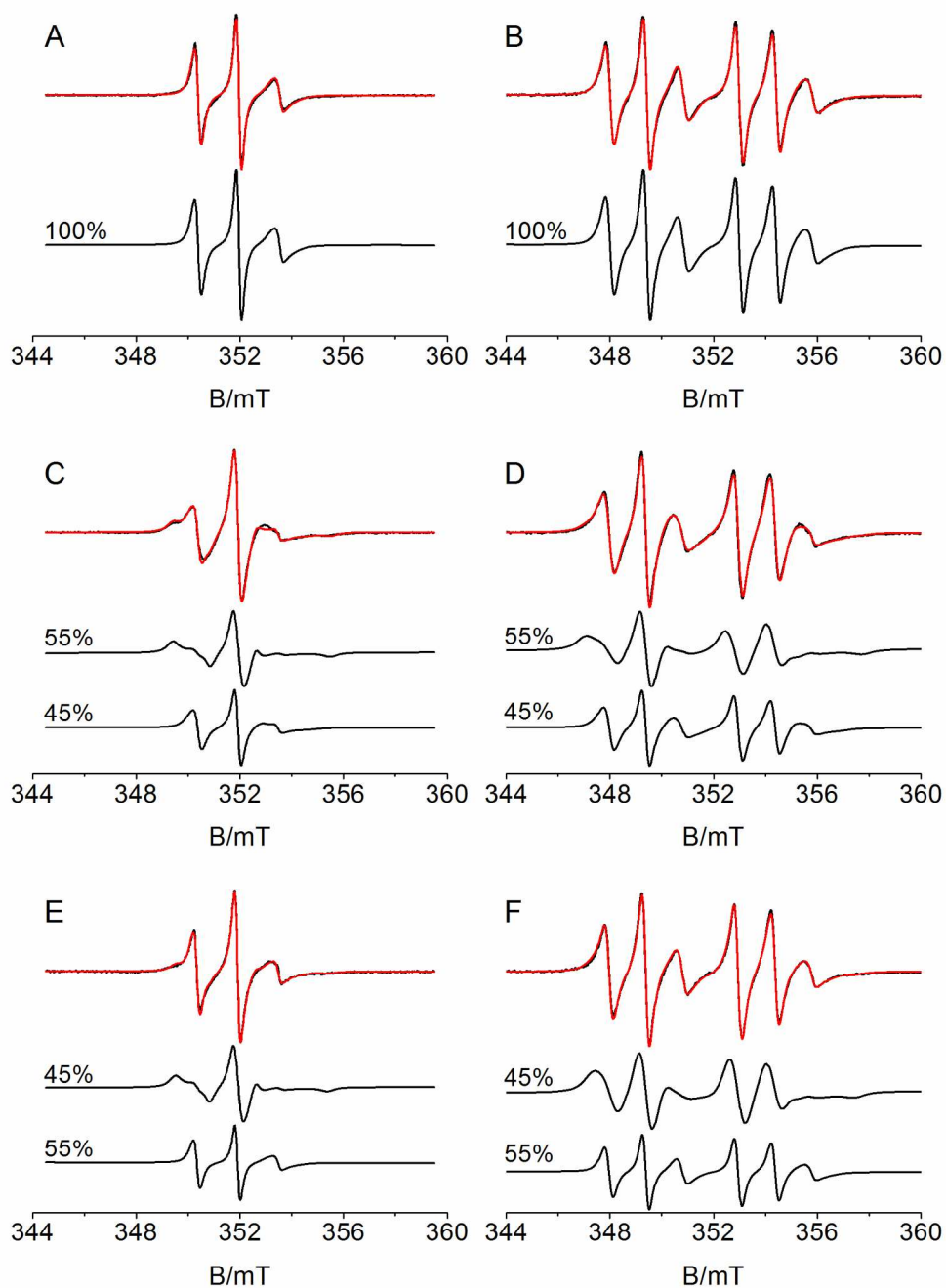
Figure S5. Amplitude normalized room temperature EPR spectra (black lines) of *(A, B)* S407C N_{TAIL} variant labeled with *(A)* P and *(B)* PP, *(C, D)* L496C N_{TAIL} variant labeled with *(C)* P and *(D)* PP and *(E, F)* V517C N_{TAIL} variant labeled with *(E)* P and *(F)* PP in 30% sucrose (w/v). The simulated spectra (red lines) obtained using the ROKI software[4] are superimposed with the experimental one. Amplitude normalized individual components corresponding to bound and unbound forms are displayed. The the following parameters have been used for the simulations: for P : $g_\perp = 2.0068$ ($\pm$ 0.0005), $g_{//} = 2.0018$ ($\pm$ 0.0005), $A_{N\perp} = 0.70$ ($\pm$ 0.06) mT, $A_{N//} = 2.7$ ($\pm$ 0.1) mT ; for PP : $g_\perp = 2.0070$ ($\pm$ 0.0005), $g_{//} = 2.0022$ ($\pm$ 0.0005), $A_{P\perp} = 4.7$($\pm$ 0.2) mT, $A_{P//} = 5.5$ ($\pm$ 0.4) mT, $A_{N\perp} = 0.7$ ($\pm$ 0.1) mT, $A_{N//} = 3.3$ ($\pm$ 0.2) mT.

Molecular dynamics
- ***Starting coordinates***

The starting structure was taken from the X-ray structure of the XD/N_{TAIL} chimera (pdb entry 1T6O).[5] Mutants S491C and L496C were built *in silico* using Swiss-PdbViewer (aka DeepView) software,[6] by changing serine 491 or leucine 496 into cysteine.

The protonation state of each residue was assigned with respect to physiological conditions by using the H^{++} server.[7] Histidine 498 was protonated at the ε nitrogen atom. Partial charges for probes P and PP were obtained from R.E.D server.[8] C-term and N-term atoms from N_{TAIL} were capped with N-methylamine and acetyl, respectively.

For each probe, four systems were built:

-N_{TAIL} alone modified at position 491

-N_{TAIL} alone modified at position 496

-N_{TAIL} modified (with P or PP) at position 491, in the vicinity of XD. In this case, the modified N_{TAIL} (with P or PP) were manually translated ~5 Å away from XD in order to avoid steric clashes between XD and the probe and to prepare unrestrained MDs dedicated to sample the binding event between the two sub-systems.

-N_{TAIL} modified at position 496 in bound to XD built from the X-Ray structure of the chimera.

The systems were then neutralized by adding one chloride ion in the case of N_{TAIL} alone or five ions when it was in interaction with XD. Finally, the water phase was modeled as a box extended to a distance of 10 Å from any solute atom.

- ***Molecular Dynamics Simulations***

Molecular dynamic simulations were carried out with either sander or pmemd within the AMBER12 suite of programs. [*AMBER 12*, University of California, San Francisco][9] ff03 parameters were used for all amino-acids and gaff parameters were obtained with Antechamber for P and PP. P and PP charges were computed with the RED server. Periodic boundaries conditions were applied and all bonds involving hydrogen atoms were constrained by using the SHAKE algorithm. A time step of 2 fs was used. An 8 Å cut-off was applied to non-bonded van der Waals interactions and the non-bonded pair list was updated every 15 steps. Particle Mesh Ewald parameters were chosen to obtain a grid spacing close to 1 Å and a 9 Å direct space cut-off.

A series of simulations described further were performed to relax water molecules and remove close contacts. 10000 steps of minimisation followed by 20 ps of Molecular Dynamics (MD) simulation with constraints (20 kcal/(mol.Å²)) applied on the solute atoms. These calculations were repeated 3 times, reducing the restraints by 5 kcal/(mol.Å²) at each round. Then, 10000 steps of minimisation without any restraint were carried out. Further, the system was slowly heated from 0 to 300 K over a period of 14 ps, using a Langevin thermostat (with a damping constant of 2 ps^{-1}), respectively. The system was then equilibrated in NVT conditions during 2 ns. An additional 10 ns equilibration simulation was carried out in NPT conditions. Finally 100 ns production with NPT conditions was performed for each structure.

To simulate the association of $N_{TAIL\_491\_PP}$ with XD, a different protocol was used. After having energy minimised the system, several MDs (10 for PP and 3 for P) simulations with different initial velocities were run for 10 ns. In 3 out of the 10 systems for PP, and 3 out of the 3 systems for P, a binding event was observed within the allowed time, with final structures showing N_{TAIL} bound to XD in a position equivalent to that of the Chimera. One typical structure of each system was selected for a further 100 ns MD run.

- ***Analysis***

Atomic fluctuations:

The quantification of the probe mobility was estimated by the atomic fluctuations of the radical oxygen atom. The 100 ns trajectory was imaged and centered on the initial structure. Rotations and translations of the system were removed by fitting the coordinate to the first structure of the trajectory. Then the atomic fluctuations were calculated for all the atoms of the probe.

Binding event:

The RMSd between the crystal structure and the structure observed during the unconstrained simulation (heating, equilibration and production phase) was calculated on the trajectory centered on the P_{XD} X-Ray structure, using VMD RMSd trajectory tools. The results are presented figures S6 and S7. The RMS deviation rapidly falls into the 2-3 Å range, emphasizing structures closely related to that of the X-Ray of the chimera. Figure S7 shows a top view of the comparison between the complexes and the chimera X-ray structure.
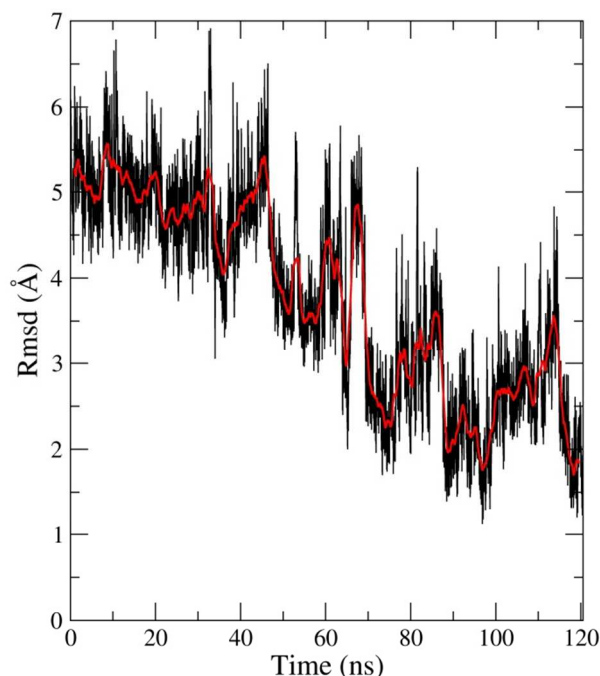
Figure S6. Root Mean Square deviation with respect to the X-Ray structure (on all atoms except hydrogen atoms) of N_{TAIL} modified with the probe P at position 491, during the whole simulation (heating phase, equilibration and production) with XD. The red curve is a running average over 100 points. The binding process is initiated by a contact between the hydrophobic residues of the $N_{TAIL\_491\_P}$ C-term and XD. The first contact is observed in the early phase of the equilibration process, after 7 ns.
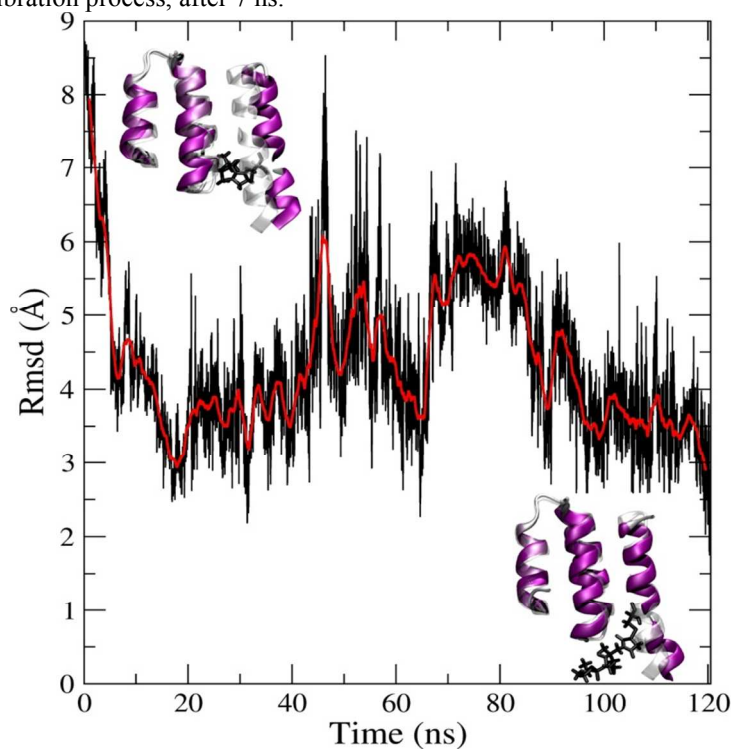

Figure S7. Root Mean Square deviation with respect to the X-Ray structure (on all atoms except hydrogen atoms) of NTAIL modified with the probe PP at position 491, during the whole simulation (heating phase, equilibration and production) with XD. The red curve is a running average over 100 points. The binding process between $N_{TAIL\_491\_PP}$

and XD occurs in the early beginning phase of the equilibration process (after 5 ns). A comparison with the X-Ray structure (in white) is provided. PP is shown in black.
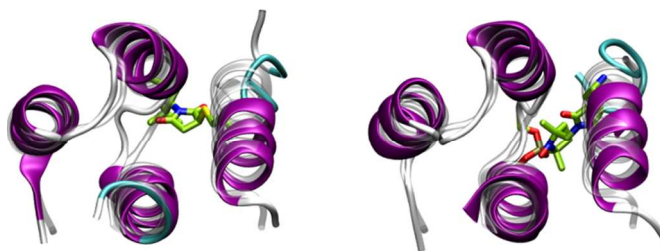

Figure S8. Top views of a typical structure of P_{XD}/N_{TAIL} S491C^P (left) and S491C^{PP} (right) sampled during the 100 ns MD. The structures are superimposed with the X-Ray structure (in white). PP and P are shown in licorice. The colors are as follows: O: red; C: green; N: blue, S: yellow, P: tan; α-helix: magenta; coil: blue

References

[1]   G. Rosini, E. Marotta, M. Petrini, R. Ballini, *Tetrahedron* **1985**, *41*, 4633-4638.
[2]   P. Baeckstrom, L. Li, I. Polec, C. R. Unelius, W. R. Wimalasiri, *Journal of Organic Chemistry* **1991**, *56*, 3358-3362.
[3]   F. Lemoigne, A. Mercier, P. Tordo, *Tetrahedron Letters* **1991**, *32*, 3841-3844.
[4]   A. Rockenbauer, L. Korecz, *Applied Magnetic Resonance* **1996**, *10*, 29-43.
[5]   R. L. Kingston, D. J. Hamel, L. S. Gay, F. W. Dahlquist, B. W. Matthews, *Proc. Nat. Acad. Sci. U. S. A.* **2004**, *101*, 8301-8306.
[6]   N. Guex, M. C. Peitsch, *Electrophoresis* **1997**, *18*, 2714-2723.
[7]   a) J. C. Gordon, J. B. Myers, T. Folta, V. Shoja, L. S. Heath, A. Onufriev, *Nucleic Acids Res* **2005**, *33*, W368-371; b) R. Anandakrishnan, A. Onufriev, *J Comput Biol* **2008**, *15*, 165-184.
[8]   a) E. Vanquelef, S. Simon, G. Marquant, E. Garcia, G. Klimerak, J. C. Delepine, P. Cieplak, F. Y. Dupradeau, *Nucleic Acids Res* **2011**, *39*, W511-517; b) F. Y. Dupradeau, A. Pigache, T. Zaffran, C. Savineau, R. Lelong, N. Grivel, D. Lelong, W. Rosanski, P. Cieplak, *Phys Chem Chem Phys* **2010**, *12*, 7821-7839.
[9]   A. W. Gotz, M. J. Williamson, D. Xu, D. Poole, S. Le Grand, R. C. Walker, *J Chem Theory Comput* **2012**, *8*, 1542-1555.

Phosphorylated nitroxide as a new spin label